SUPPLEMENTARY MATERIALS AND METHODS

Immunofluorescence.

Cells were fixed in cold 4% paraformaldehyde for 15 min, rinsed and stored at +4 °C prior to analysis. Primary antibody staining was performed for Nestin (mouse, 1:200, Millipore, Billerica, MA), Tuj-1 (mouse, 1:1000, Covance, Princeton, NJ) and Ki67 (mouse, 1:200, Dako, Glostrup, Denmark). After incubation, cells were washed and incubated with species-specific secondary antibodies conjugated to Alexa dyes (Invitrogen, Carlsbad, CA). Cells were counterstained with DAPI to measure total cell number. Staining was visualized by epifluorescence (Vico, Nikon, Melville, NY) or confocal epifluorescence microscopy (Ti-E-A1, Nikon, Melville, NY).

Luciferase reporter assays.

GBM cells were transfected using Effectene Reagent (Qiagen, Hilden, Germany). BAT-luciferase reporter construct (BAT-lux) consists of seven TCF/LEF-binding sites upstream of a 0.13-kb fragment containing the minimal promoter–TATA box of the gene *siamois* (1), driving the expression of the firefly luciferase reporter gene. The hypoxia luciferase reporter assay was performed by using an HRE-luciferase reporter construct (wHRE) consisting of a trimerized 24-mer containing 18 bp of sequence from the PGK promoter including the HRE (5'-tgtcacgtcctgcacgactctagt, HRE) and an 8 bp linker sequence followed by a 50 bp minimal tyrosine kinase promoter in a pGL2-firefly luciferase Basic Vector backbone (Promega, Madison, WI).

The Notch luciferase reporter assay was performed using a reporter plasmid (6x-RBP-Jk-luc) containing six copies of the CBF1 binding consensus sequence (5'-tgggaa, Notch consensus sequence) from the Hes1 promoter used to evaluate Notch-mediated transcription. In all cases, transfection with a Renilla luciferase vector was used in order to normalize luciferase detection (Promega, Madison, WI).

Twenty-four hours after transfection, a total medium change was carried out, and cells were treated with 30 ng/ml of soluble Wnt3a and maintained at 2% O_2 or acutely expose to 20% O_2. Where

indicated, GBM-derived cells were co-transfected with CA-β-catenin plasmid or pcDNA3.1:NICD. Cells were processed for analysis of BAT-lux, HRE- and Notch-luciferase activity as described in the kit (Dual-Luciferase Reporter Assay System, Promega, Madison, WI) using a plate-reading luminometer (Victor, Perkin Elmer, Waltham, MA). Values reported in the graphs are expressed in relative light units (RLU) and were normalized to the control group at 2% oxygen.

Western blot and densitometric analysis.

Total protein extracts were isolated in lysis buffer as described previously (2, 3). Equal amounts of protein (10–20 μg) were resolved using an SDS-PAGE gel (Criterion, Bio-Rad, Hercules, CA) and transferred to PVDF Hybond-p membrane (GE Healthcare, London, Canada). Membranes were blocked with I-block^{TM} Blocking (Tropix, Sigma-Aldrich, St. Louis, MO) for at least 1 hour or overnight, under rotation at RT or 4 °C. Membranes were then incubated overnight at 4 °C under constant shaking for NUMB PAN-ISO (rabbit, 1:500, Upstate biothecnology, Lake Placid, NY), NUMB-L (rabbit, 1:1000, Novus Biologicals, Littleton, CO), Notch1 (rabbit, 1:1000, Cell Signalling Technologies Inc., Beverly, MA), Dll4 (rabbit, 1:500, Abcam, Cambridge, UK), Hes1 (rabbit, 1:250, Chemicon, Billerica, MA), phospho-β-catenin (Ser33/37/Th41; rabbit, 1:1000, Cell Signalling Technologies Inc., Beverly, MA); total β-catenin (rabbit, 1:5000, Abcam, Cambridge, UK), phospho-GSK3α/β (Ser21/9, rabbit, 1:1000, Cell Signalling Technologies Inc., Beverly, MA), $p21^{cip1}$ (mouse, 1:1000, Sigma-Aldrich, St. Louis, MO), TCF-1 (rabbit, 1:100, Cell Signalling Technologies Inc., Beverly, MA), TCF-4 (rabbit, 1:1000, Cell Signalling Technologies Inc., Beverly, MA) and β-actin (mouse, 1:10000, Sigma-Aldrich, St. Louis, MO) as loading control.

Membranes were next incubated with peroxidase-labelled goat anti-rabbit or anti-mouse IgG (1:100.000; Sigma-Aldrich, St. Louis, MO) for 60 min. All membranes were visualized using ECL Advance (GE Healthcare, London, Canada) and exposed to Hyperfilm MP (GE Healthcare, London, Canada). Densitometric analysis of the films was performed using Image J software.

Real-Time PCR analysis.

RNA was isolated from GBM cells or zebrafish larval brains using Trizol (Invitrogen, Carlsbad, CA) and 0.5 μg of total RNA reverse-transcribed using SuperScriptRNAse H-Reverse Transcriptase (Invitrogen, Carlsbad, CA). Quantitative RT-PCR reactions were run in triplicate using a Brilliant® SYBR® Green QPCR Core Reagent Kit (Stratagene, La Jolla, CA). Fluorescent emission was recorded in real-time (Sequence Detection System 7900HT, Applied Biosystems, Carlsbad, CA). Gene expression analysis was completed using the comparative Ct method of relative quantification. PCR amplification conditions consisted of 40 cycles with primers annealing at 60 °C. Sequences of specific primers used in this work are listed in Supplementary Table S3.

Primers were designed using the software Primer 3 (http://frodo.wi.mit.edu/primer3/input.htm), and the specificity of the primers for the human sequences was evaluated using the software Human BLAT Search (http://genome.ucsc.edu/cgi-bin/hgBlat?command=start). PCR amplicons had been previously evaluated on agarose gel (see Suppl. Table S3), and during SYBR green analyses, primer dissociation curves were checked in each run to ensure primer specificity to human mRNA. Relative RNA quantities were normalized to *GUSB*, and human GBM cells prior to injection were used as the calibrating condition (ΔΔCt Method).

Transduction of GBM derived cells using lentiviral vectors.

The lentiviral plasmids containing HIF-1α siRNA and Luciferase (Luc) siRNA target sequences, termed pLSLG-HIF-1α-siRNA and pLSLG-Luciferase-siRNA, respectively, were a kind gift of Dr. O.V. Razorenova (Department of Molecular Cardiology, Lerner Research Institute, Cleveland, OH). The lentiviral vectors were produced as previously described (2) and used to infect GBM cells. Efficiency of transduction was evaluated by flow-cytometry (FC500 Beckman Coulter, Brea, CA).

Labelling of human cells with vital dye.

Cell pellets were resuspended at a density of 1×10^6 cells/ml in serum-free DMEM/F12 (Irvine Scientific, Irvine, CA); then the cell-labelling solution (Vibrant-DiI or Vibrant-DiO; Invitrogen, Carlsbad, CA) was added for a final concentration of 5 μM. Cells were gently mixed and incubated for 20 minutes at 37 °C in the dark. The labelled suspension tubes were centrifuged at 1150 rpm for 7 minutes. The supernatant was removed, and the pellet was gently resuspended in warm (37 °C) serum-free medium. The wash procedure was repeated two more times. Finally, cells were resuspended in complete medium at a final concentration of 10^7 cells/ml.

Live Imaging of zebrafish embryos/larvae.

Xeno-transplanted zebrafish live larvae and reporter zebrafish were anaesthetized with Tricaine (0.5 mM 3-aminobenzoic acid ethyl ester; Sigma-Aldrich, St. Louis, MO) and then embedded in 1% low melting agarose in methylene blue free fishwater, with Tricaine added. Images and stacks were acquired using a Biorad confocal microscope, and images or 3D reconstruction were processed for figures and videos using ImageJ software (Research Services Branch, National Institute of Mental Health, Bethesda, Maryland, USA.).

Zebrafish immunofluorescence and in situ hybridization.

Xeno-transplanted zebrafish larvae were fixed in 4% paraformaldehyde, paraffin-embedded and cut in 5 μm-thick sections. Sections were re-hydrated, and then antigen retrieval was performed by incubation in citrate buffer 0.01 M, pH6, at 95 °C for 20 min. After saturation with 5% BSA, slides were incubated with anti-Nestin (mouse, 1:100, Chemicon, Billerica, MA), anti-Tuj-1 (mouse, 1:500, Covance, Princeton, NJ), anti-MAP2 (mouse, 1:100, Sigma-Aldrich, St. Louis, MO) and anti-Ki67 (mouse, 1:200, Dako, Glostrup, Denmark). After incubation, sections were washed and incubated with species-specific secondary antibodies conjugated to Alexa dyes (1:1000, Invitrogen, Carlsbad, CA). The specificity of each staining procedure was confirmed by replacing the primary antibodies with the specific isotype control. Tissues were counterstained with DAPI (1:10000,

Sigma-Aldrich, St. Louis, MO) to evidence cell nuclei and zebrafish morphology. Staining was visualized by epifluorescence (Vico, Nikon, Melville, NY), and images processed for figures using Adobe Photoshop or Illustrator (Adobe, San Jose, CA). In situ hybridization was performed as described (4).

Statistical analysis

Graphs and statistical analyses were prepared using Prism 4.00 (Graph Pad, La Jolla, CA). All values are presented as mean ± standard error of the mean (S.E.M.). Statistical significance was measured by one-way ANOVA with Newman-Keuls multiple comparison post Test, *$p<0.05$, **$p<0.01$, ***$p<0.001$.

References

1. Maretto S, Cordenonsi M, Dupont S, Braghetta P, Broccoli V, Hassan AB*, et al.* Mapping Wnt/beta-catenin signaling during mouse development and in colorectal tumors. *Proc Natl Acad Sci U S A* 2003 Mar 18; 100(6): 3299-3304.

2. Pistollato F, Chen HL, Rood BR, Zhang HZ, D'Avella D, Denaro L*, et al.* Hypoxia and HIF1alpha repress the differentiative effects of BMPs in high-grade glioma. *Stem Cells* 2009 Jan; 27(1): 7-17.

3. Pistollato F, Rampazzo E, Abbadi S, Della Puppa A, Scienza R, D'Avella D*, et al.* Molecular mechanisms of HIF-1alpha modulation induced by oxygen tension and BMP2 in glioblastoma derived cells. *PLoS One* 2009; 4(7): e6206.

4. Moro E, Ozhan-Kizil G, Mongera A, Beis D, Wierzbicki C, Young RM*, et al.* In vivo Wnt signaling tracing through a transgenic biosensor fish reveals novel activity domains. *Dev Biol* 2012 Jun 15; 366(2): 327-340.

SUPPLEMENTARY TABLES S1-3

Supplemental Table S1

GBM Tumors used in study

Code	*Classification*	*Age (y)*	*Gender*
HuTu01	Glioblastoma	65	male
HuTu10	Glioblastoma	75	female
HuTu13	Glioblastoma	67	male
HuTu15	Glioblastoma	76	female
HuTu47	Glioblastoma	80	female
HuTu53	Glioblastoma	70	male
HuTu63	Glioblastoma	37	female
HuTu83	Glioblastoma	55	male
HuTu102	Glioblastoma	40	male
HuTu107	Glioblastoma	65	male
HuTu155	Glioblastoma	48	female

Supplementary Table S2

Down-regulated probe sets along the 3 time points in the intersection list

Probe sets	***Gene Symbol***
1556499_s_at	*COL1A1*
200077_s_at	*OAZ1*
200599_s_at	*HSP90B1*
200650_s_at	*LDHA*
200738_s_at	*PGK1*
200771_at	*LAMC1*
200773_x_at	*LOC643287 /// PTMA*
200807_s_at	*HSPD1*
200832_s_at	*SCD*
200858_s_at	*RPS8*
200886_s_at	*hCG_2015138 /// PGAM1*
200958_s_at	*SDCBP*
200966_x_at	*ALDOA*
201005_at	*CD9*
201105_at	*LGALS1*
201426_s_at	*VIM*
201464_x_at	*JUN*
201645_at	*TNC*
201667_at	*GJA1*
201669_s_at	*MARCKS*
201849_at	*BNIP3*
201938_at	*CDK2AP1*
202403_s_at	*COL1A2*
202404_s_at	*COL1A2*
202428_x_at	*DBI*
204170_s_at	*CKS2*
204469_at	*PTPRZ1*
204471_at	*GAP43*
205029_s_at	*FABP7*
205030_at	*FABP7*
205292_s_at	*HNRNPA2B1*
208628_s_at	*YBX1*
208636_at	*ACTN1*
208752_x_at	*NAP1L1*
208892_s_at	*DUSP6*
208894_at	*HLA-DRA*
209189_at	*FOS*
209389_x_at	*DBI*
209465_x_at	*PTN*
209466_x_at	*PTN*
209656_s_at	*TMEM47*
210139_s_at	*PMP22*
210512_s_at	*VEGFA*
210561_s_at	*WSB1*
211070_x_at	*DBI*
211737_x_at	*PTN*
211943_x_at	*TPT1*

211945_s_at	*ITGB1*
211959_at	*IGFBP5*
211990_at	*HLA-DPA1*
212284_x_at	*TPT1*
213011_s_at	*TPI1*
213084_x_at	*hCG_16001 /// hCG_2001000 /// RPL23A*
213428_s_at	*COL6A1*
213881_x_at	*SUMO2*
213911_s_at	*H2AFZ*
217398_x_at	*GAPDH*
217757_at	*A2M*
217871_s_at	*MIF*
221479_s_at	*BNIP3L*
221841_s_at	*KLF4*
224606_at	*KLF6*
225413_at	*USMG5*
225540_at	*MAP2*
226189_at	*ITGB8*
37892_at	*COL11A1*

Probe sets with down regulation at 24 hpi time point and upregulation at 48 hpi time point

Probe sets	***Gene Symbol***
200665_s_at	*SPARC*
201550_x_at	*ACTG1*
201876_at	*PON2*
207030_s_at	*CSRP2*
210198_s_at	*PLP1*
210968_s_at	*RTN4*
211719_x_at	*FN1*
214629_x_at	*RTN4*
221607_x_at	*ACTG1*
224585_x_at	*ACTG1*
200638_s_at	*YWHAZ*
208640_at	*RAC1*
210211_s_at	*HSP90AA1*

Up-regulated probe sets along the 3 time points in the intersection list

Probe sets	***Gene symbol***
209167_at	*GPM6B*
209170_s_at	*GPM6B*
209283_at	*CRYAB*
212097_at	*CAV1*
214247_s_at	*DKK3*
219087_at	*ASPN*
221805_at	*NEFL*
221916_at	*NEFL*

Supplementary Table S3

Sequence of primers used in this study

Gene	*Sequence (5'-3')*	*Amplicon (bp)*
MAP2 forward	GGGTCACAGGGCACCTATTC	129
MAP2 reverse	GCTACAGCCTCAGCAGTGAC	
β-III-tubulin (Tuj1) forward	GGGGCCTTTGGACATCTCTT	126
β-III-tubulin (Tuj1) reverse	CACCACATCCAGGACCGAAT	
Neuro D1 forward	CAGACGAGTGTCTCAGTTCTCA	139
Neuro D1 reverse	TCCTCTTCCAGGTCCTCATCTT	
Neurogenin 1 forward	CCCCTAGTCAGCAGGCAATA	72
Neurogenin 1 reverse	GGTCAGTTCTGAGCCAGTC	
LDHA forward	GGCCTGTGCCATCAGTATCT	177
LDHA reverse	ACCAGCTTGGAGTTTGCAGT	
VEGF forward	AACCATGAACTTTCTGCTGTCT	129
VEGF reverse	TTCACCACTTCGTGATGATTCT	
DKK3 forward	GCCTGGTGTATGTGTGCAAG	91
DKK3 reverse	TCATACTCATCGGGGACCTC	
GPM6B forward	GCTGGGTGTGTTTGGTTTCT	84
GPM6B reverse	TGCGGTGACTTGATGACTTC	
JUN forward	CCAAGAACTCGGACCTCCT	96
JUN reverse	CCCGTTGCTGGACTGGATTA	
KLF4 forward	CTGCGGCAAAACCTACACAA	90
KLF4 reverse	CGTCCCAGTCACAGTGGTA	
Numb forward	GTCGCTGGATCTGTCACTGCT	102
Numb reverse	TCTGCTTGCGCTCTAAACAGG	
NumbLike forward	CCTTTCAAACGGCAGCTGAG	102
NumbLike reverse	AGGCTCCATCTCAGGCACTG	
Numb-1180_forward	GCTAGTAGGGCTATTTAAGAACTGC	136
Numb-1180_reverse	GCCCGGCCAGCAACTTTCTAATA	
Numb-418_forward	GCAGGAAGTGAGCTGGAGAAG	118
Numb-418_reverse	GCGCAGTAGAAAGCAAAGGAG	
TCF-1 forward	CCTAGCAAGGAGGAGCGAGA	143
TCF-1 reverse	CCGGTTGGCAAACCAGTTGTAG	
TCF-3 forward	AAGAAGCCCCACGTGAAGAAG	133
TCF-3 reverse	GGTTGTGCCACTTTCTTCCAAGGA	
TCF-4 forward	TTTAAGGGGCCACCGTATCC	119
TCF-4 reverse	TGCCGGACTGAAAATGGAG	
LEF-1 forward	TCTCAGGAGCCCTACCACGA	94
LEF-1 reverse	CGAGTAGGAGGGTCCCTTGTT	
β-glucuronidase (GUSB) forward	GAAAATACGTGGTTGGAGAGCTCATT	101
β-glucuronidase (GUSB) reverse	CCGAGTGAAGATCCCCTTTTTA	

SUPPLEMENTARY FIGURES S1-10

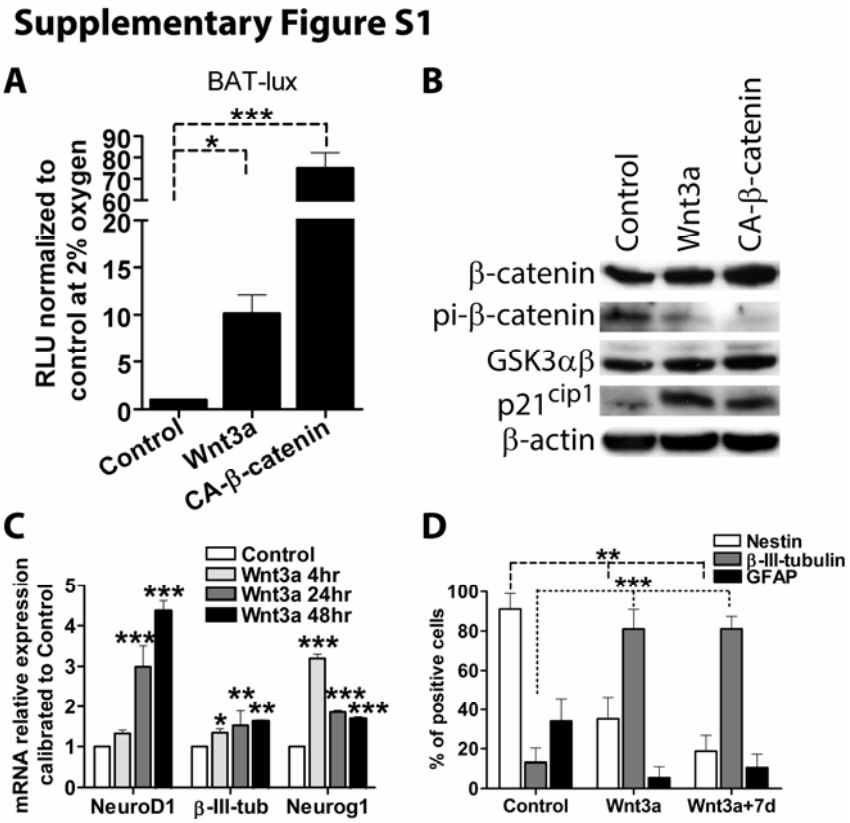

Supplementary Figure S2

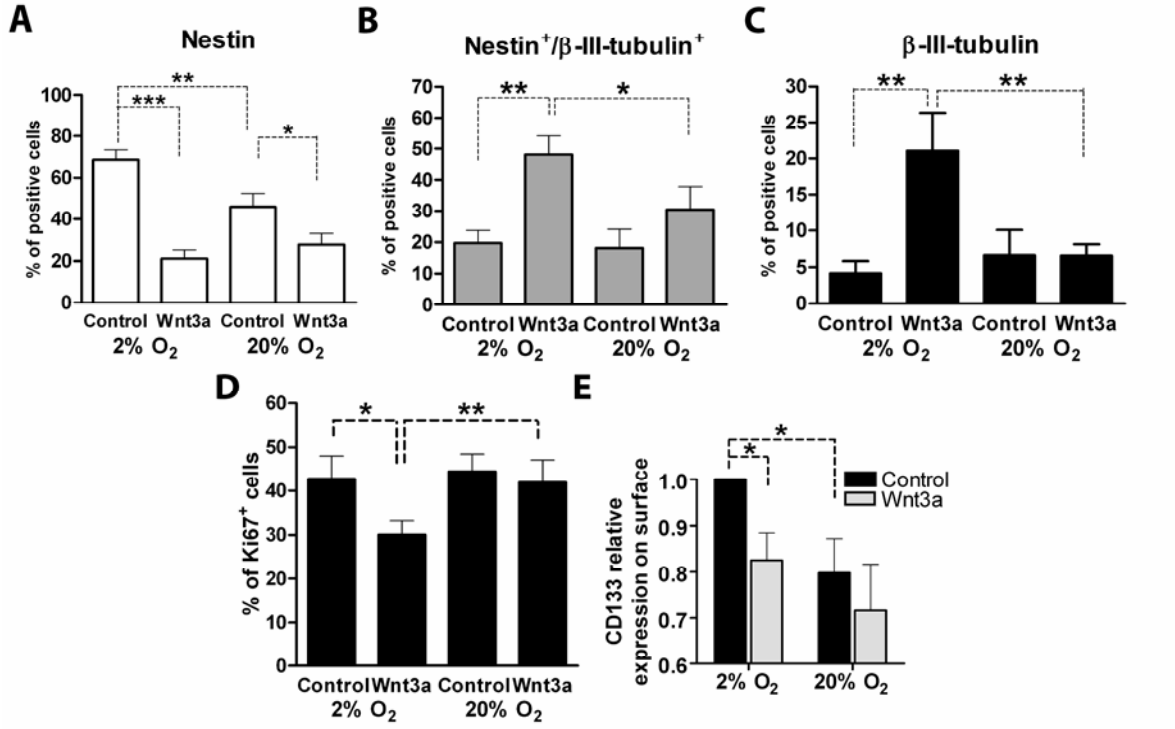

Supplementary Figure S3

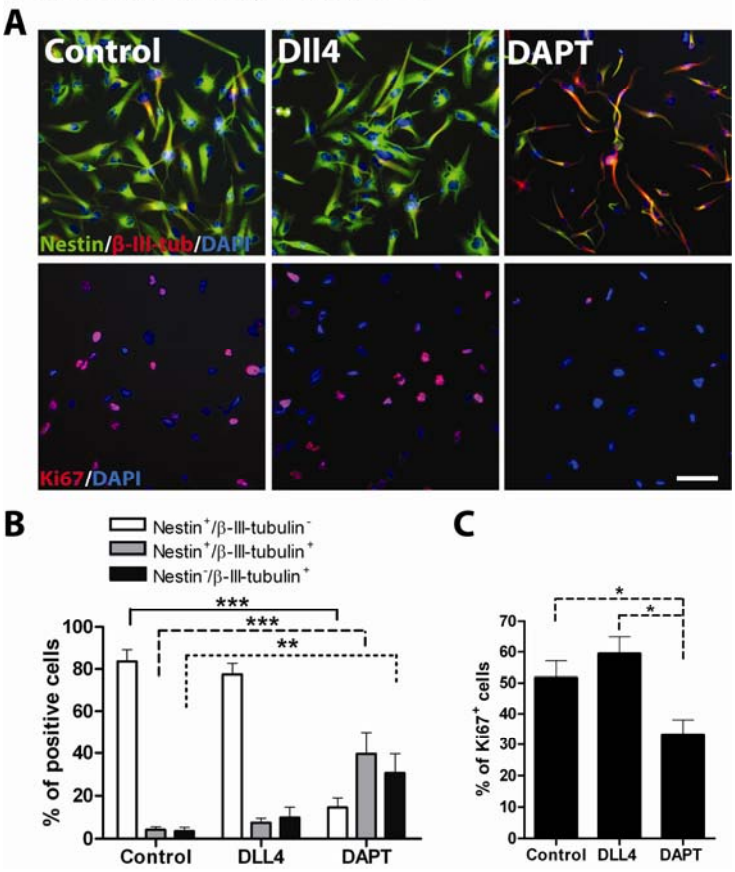

Supplementary Figure S4

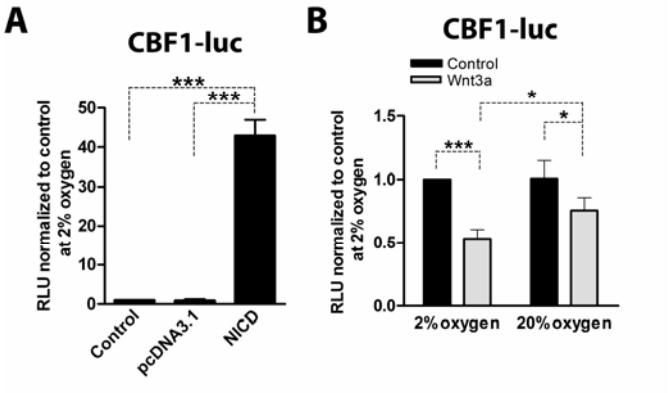

Supplementary Figure S5

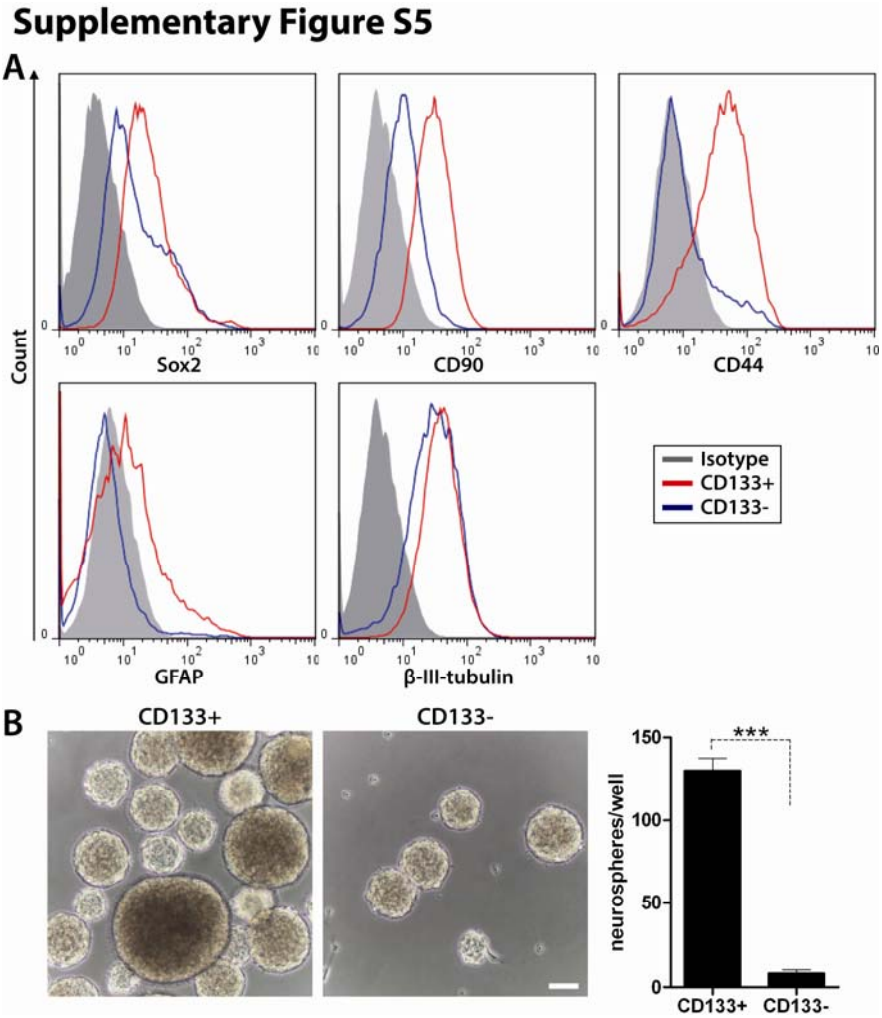

Supplementary Figure S6

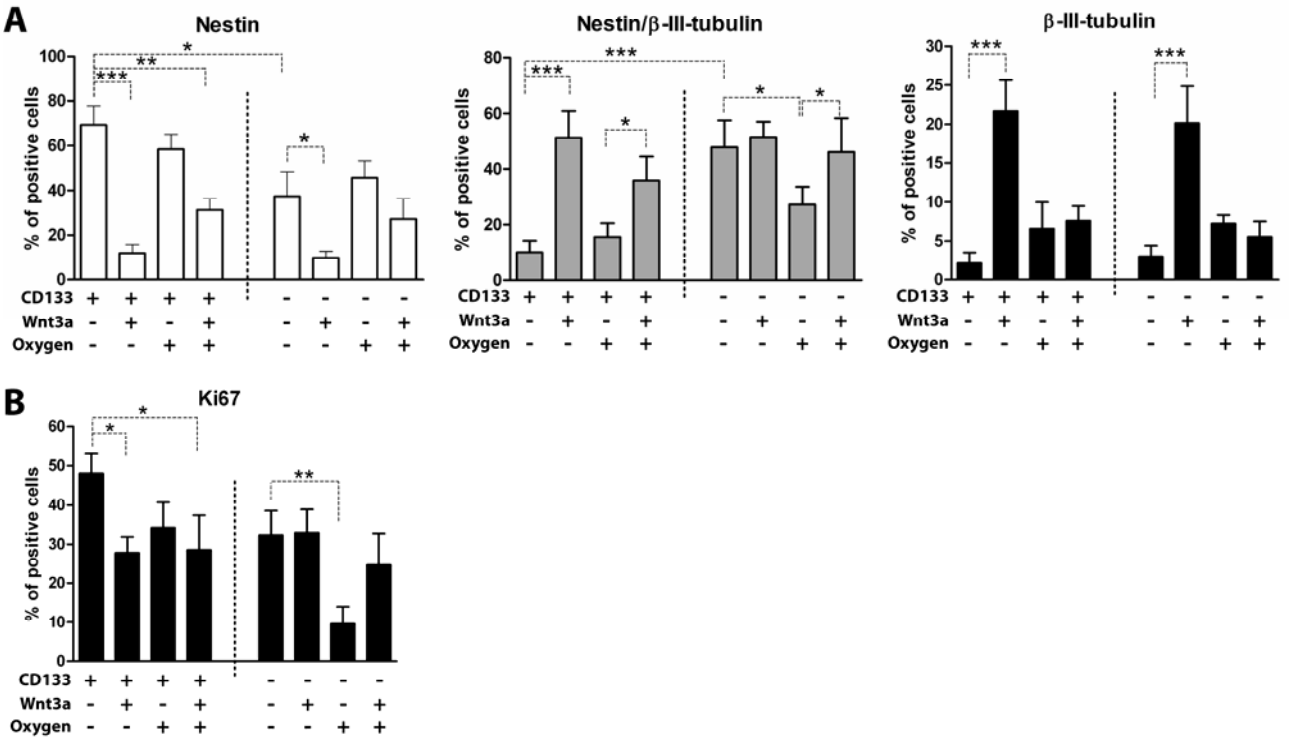

Supplementary Figure S7

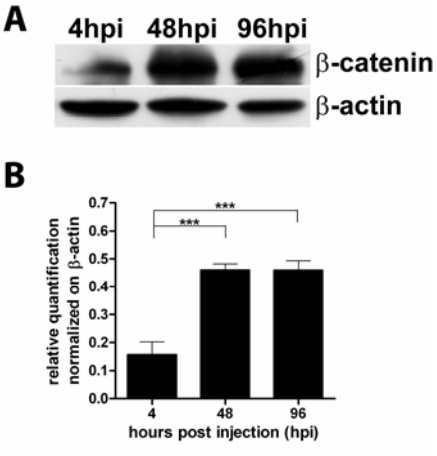

Supplementary Figure S8

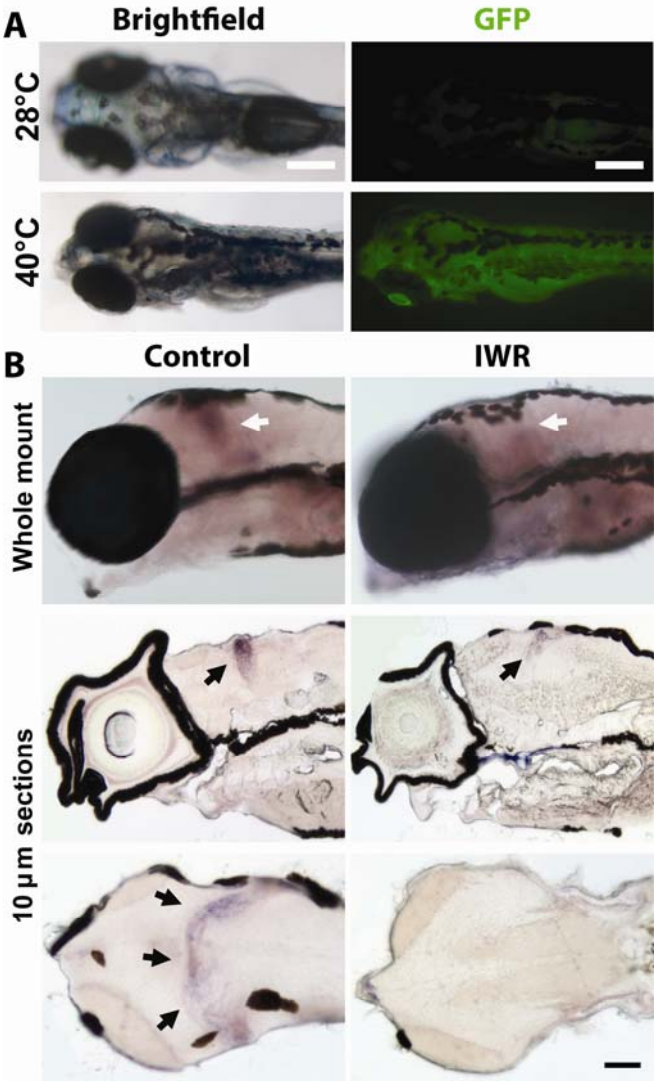

Supplementary Figure S9

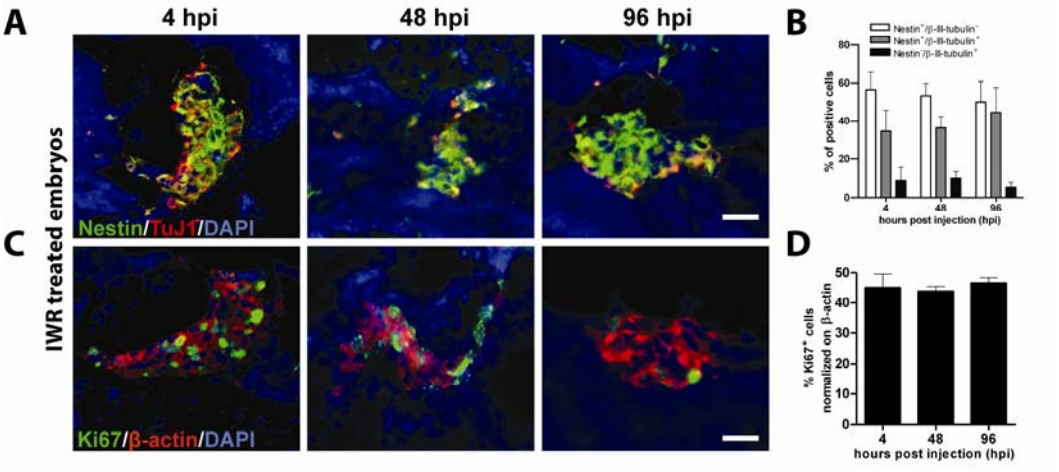

Supplementary Figure S10

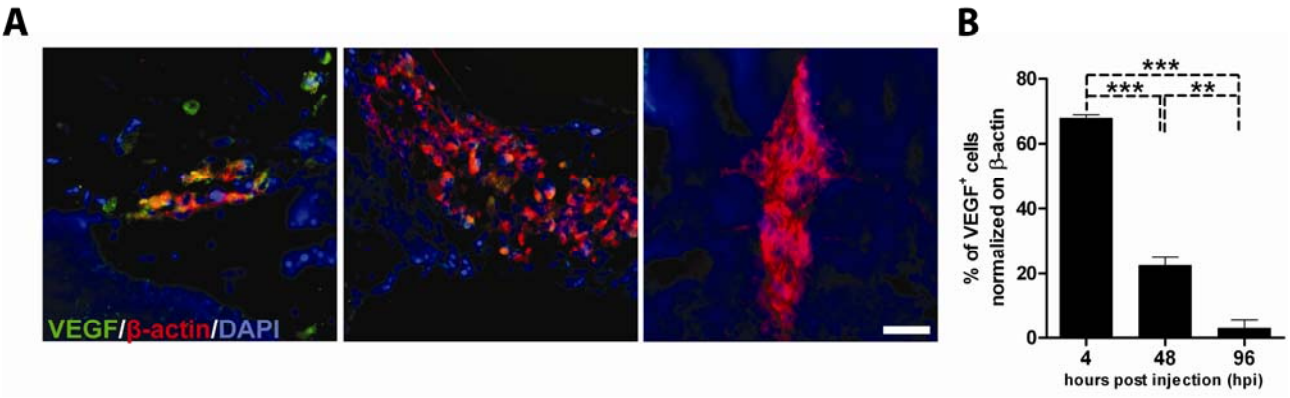

SUPPLEMENTARY FIGURE LEGENDS

Supplementary Figure S1. Canonical Wnt3a induces neuronal differentiation of GBM derived cells. (**A**) BAT-lux reporter analysis of Wnt3a-treated or CA-β-catenin-transfected cells at 2% O_2. Mean of 3 tumours ± S.E.M., n=2 for each tumour. (**B**) WB representing the activation status of β-catenin, its regulator GSK3αβ and the differentiation /proliferation marker $p21^{cip1}$ of GBM cells treated with Wnt3a or transfected with CA-β-catenin plasmid. Analysis repeated on additional 3 tumours. (**C**) RQ-PCR analysis showing mRNA levels of NeuroD1, β-III-tubulin and Neurog1. Mean of 6 different tumours, n=4 for each tumour. (**D**) Bar graph reporting relative quantification of immunofluorescence images of GBM cells treated with Wnt3a or after Wnt3a withdrawal and stained for Nestin (green)/β-III-tubulin (red). Mean of 3 tumours ± S.E.M. n=2 for each tumour. *p<0.05, **p<0.01, ***p<0.001.

Supplementary Figure S2. Hypoxia modulates Wnt signalling activation in GBM-derived cells. (**A-D**) Bar graphs reporting relative quantification of $Nestin^+$/β-III-$tubulin^-$, $Nestin^+$/β-III-$tubulin^+$ and $Nestin^-$/β-III-$tubulin^+$ sub-populations of Wnt3a-treated GBM cells at different oxygen tensions. (**E**) Analysis of CD133 cell surface marker expression after Wnt3a treatment of 2% or 20% O_2 cultured cells. Mean of 5 tumours ± S.E.M., n=2 for each tumour. *p<0.05, **p<0.01, ***p<0.001.

Supplementary Figure S3. Notch signalling inhibition promotes neuronal differentiation of GBM-derived cells. (**A**) Representative immunofluorescence images of GBM cells treated with Dll4 or DAPT for 96h and stained for Nestin (green)/β-III-tubulin (red) and Ki67 (red). Bar=100 μm. (**B-C**) Bar graph reporting relative quantification of images described in panel (**A**). Mean of 3 tumours ± S.E.M. n=3 for each tumour. *p<0.05, **p<0.01, ***p<0.001.

Supplementary Figure S4. CBF1-luc analysis on GBM-derived cells. (**A**) CBF1-luc luciferase assay on NICD transfected or control cells. (**B**) CBF1-luc luciferase assay conducted on Wnt3a-treated GBM cells at different oxygen tensions. For all graphs, mean of 3 tumours ± S.E.M., n=2 for each tumour. *p<0.05, **p<0.01, ***p<0.001.

Supplementary Figure S5. Low oxygen tension enhances Wnt-dependent differentiation only in CD133$^+$ GBM-derived cells. (**A**) Bar graphs reporting relative quantification of Nestin$^+$/β-III-tubulin$^-$, Nestin$^+$/β-III-tubulin$^+$ and Nestin$^-$/β-III-tubulin$^+$ sub-populations of CD133$^+$ and CD133$^-$ sorted cells treated or not treated with Wnt3a at different oxygen tensions. (**B**) Bar graph showing % of Ki67$^+$ cells treated as in panel (**A**). For all graphs, mean of 3 tumours ± S.E.M., n=10 for each tumour. *p<0.05, **p<0.01, ***p<0.001.

Supplementary Figure S6. Phenotypic and functional characterization of CD133$^+$ GBM derived cells. (**A**) Cytofluorimetric analyses of stemness (Sox2, CD90, and CD44) and differentiation (GFAP and β-III-tubulin) markers expression in CD133$^+$ (red line) and CD133$^-$ (blue line) GBM cells. (**B**) Representative images showing neurospheres generated from CD133$^+$ and CD133$^-$ sorted GBM cells plated in non-coated dishes at a concentration of 1000 cells/P12 well and relative quantification. Bar=200μm. ***p<0.001.

Supplementary Figure S7. Wnt pathway is activated in GBM cells *in vivo*. (**A**) Representative western blot analyses of human β-catenin in total protein extracts retrieved from zebrafish brains transplanted with GBM cells after 4, 48 and 96hpi along with human β-actin as loading control. (**B**) Bar graph reporting relative β-catenin protein quantification normalized to human β-actin. The analysis has been confirmed on additional 3 tumours. For the graph, mean of 4 tumours ± S.E.M., n=3 for each tumour. *p<0.05, **p<0.01, ***p<0.001.

Supplementary Figure S8. GFP expression after *hsp70l:dkk1-GFP* larvae heat-shock and Neurod expression in IWR-treated zebrafish larvae. (**A**) Representative images of *hsp70l:dkk1-GFP* larvae maintained at 28°C (upper panels) and after heat shock (40 °C) (lower panels). Left panels: live larvae; right panel: transgene expression after heat shock. bar=100μm. (B) Representative images of *neurod* expression by whole mount in situ hybridization on control and IWR-treated (72h) zebrafish larvae at 9dpf. Arrows indicate sites of *neurod* expression. Larvae were OCT-embedded and sectioned post–staining. The analysis has been confirmed in 3 independent experiments on 150 larvae. Bar=100μm.

Supplementary Figure S9. Wnt pathway suppression blocks transplanted GBM cell differentiation. (**A**,**C**) Representative immunofluorescence images of IWR-treated xeno-transplanted larvae stained for Nestin (green)/β-III-tubulin (red) (**A**) and Ki67 (green)/β-actin (red) (**C**). (**B**,**D**) Relative quantification of images described in (**A**,**C**).

Supplementary Figure S10. Validation of GEP data. (**A-B**) Representative immunofluorescence images of paraffin-embedded tissue sections of xeno-transplanted zebrafish larvae at 4, 48 and 96hpi stained for VEGF (green)/β-actin (red) (**A**) and bar graphs reporting relative quantifications (**B**). Bar=40μm. Mean of 3 tumours ± S.E.M., n=4 for each tumour.